Microneedle-Mediated Transdermal Delivery of Bevacizumab

Courtenay, A. J., McCrudden, M. T. C., McAvoy, K. J., McCarthy, H. O., & Donnelly, R. F. (2018). Microneedle-Mediated Transdermal Delivery of Bevacizumab. *Molecular Pharmaceutics*, *15*(8), 3545-3556. https://doi.org/10.1021/acs.molpharmaceut.8b00544

Published in:
Molecular Pharmaceutics

Document Version:
Peer reviewed version

Microneedle Mediated Transdermal Delivery of Bevacizumab

Aaron J. Courtenay, Maelíosa T.C. McCrudden, Kathryn J. McAvoy, Helen O. McCarthy, and Ryan F. Donnelly*.

School of Pharmacy, Queen's University Belfast, Medical Biology Centre, 97 Lisburn Road, Belfast BT9 7BL, UK.

*Corresponding author
Professor Ryan F. Donnelly
Chair in Pharmaceutical Technology
School of Pharmacy
Queen's University Belfast
Medical Biology Centre
97 Lisburn Road
Belfast
BT9 7BL
UK
Tel: +44 (0) 2890 972 251
Fax: +44 (0) 2890 247 794
Email: r.donnelly@qub.ac.uk

Abstract

Bevacizumab is a recombinant humanised monoclonal antibody used clinically as a combination chemotherapeutic. Antibody therapeutics are usually formulated as parenteral injections, owing to their low oral bioavailability. Microneedle technology provides a transdermal alternative for drug-delivery using micron-scale needle structures to penetrate directly through the s*tratum corneum* into the dermal interstitium. This study describes the design, formulation and *in vitro* characterisation of both dissolving and hydrogel-forming microneedle array platforms for transdermal delivery of bevacizumab. Bevacizumab recovery and transdermal permeation studies were conducted and analysed using bevacizumab specific ELISA. Prototype microneedle-patches were tested *in vivo* in Sprague-dawley rats with serum, exterior lumbar and axial lymph nodes, spleen and skin tissue concentrations of bevacizumab reported. This work represents the first example of high dose transdermal delivery of an antibody therapeutic *in vivo* using dissolving and hydrogel-forming microneedle platforms. Basic pharmacokinetic parameters are described including hydrogel-forming microneedles: C_{max} 358.2 ± 100.4 ng/ml, T_{max} 48 h, AUC 44357 ± 4540 & C_{ss} 942 ± 95ng/ml, highlighting the potential for these devices to provide sustained delivery of antibody therapeutics to the lymph and systemic circulation. Targeted delivery of chemotherapeutic agents to the lymphatic system by MN technology may provide new treatment options for cancer metastases.

Keywords Microneedle, bevacizumab, transdermal, hydrogel-forming, dissolving.

1. Introduction

The use of biotherapeutic agents has increased rapidly in the past 10 years to become a mainstream treatment option for many diseases, such as cancer [1]. Proteins, peptides, virus-like particles and antibody therapies have progressed to such an extent that they can facilitate efficacious treatment of diseases previously not effectively managed by small molecule drugs. Bevacizumab (BEV) is a humanised monoclonal antibody therapeutic available within the European Union since its licensure in 2005 [2]. Commercially available as Avastin®, manufactured by Roche, BEV is indicated for the treatment of a number of cancers, namely: metastatic colorectal cancer, first-line treatment of advanced non-squamous non-small cell lung cancer, metastatic breast cancer, advanced renal cell carcinoma, advanced epithelial ovarian, fallopian tube and primary peritoneal cancer [3] . The efficacy of highly selective target-ligand binding molecules, such as BEV, has paved the way for therapeutic agents with minimal off-target effects, resulting in better treatments with fewer side effects [4]. However, with these added advantages have come a number of formulation challenges. Currently, BEV is available as a concentrated solution for infusion and is delivered over 30 – 90 min, using traditional needle and syringe technology. The vast majority of biotherapeutic antibody drugs like BEV are delivered in a similar way. It has been well documented that one significant drawback to biotherapeutic formulation is the lack of appropriate drug delivery platforms available for biologic drugs. Biotherapeutics are particularly prone to degradation, even under highly controlled environments. Loss of biological activity can arise as a result of structural changes resulting from variation in pH, alterations in ionic and osmotic pressure and shear stresses exerted on the formulation [5]. A number of formulation options have been explored for delivery of monoclonal antibodies, such as pulmonary and nasal delivery. However, these have failed to become widely accepted within the pharmaceutical industry and instead have remained within the realm of curiosity-driven research [6]. Similarly, significant costs associated with initial development of biotherapeutic agents, such as BEV, have made these treatment options expensive. As such, this expense has resulted in the need to develop delivery methods that demonstrate high dose-delivery efficiency.

Microneedle (MN) technology has emerged as a credible option for transdermal drug delivery of biotherapeutic agents. MN are micro-dimensional protrusions arranged on a supporting baseplate that can penetrate the skin's *stratum corneum* (*SC*) barrier and provide access for

drugs to dermal tissue. A number of research groups have demonstrated successful delivery of drug therapies across the *SC* and into the dermal microcirculation [7–9]. Polymeric MN platforms such as dissolving and hydrogel-forming systems show most promise with respect to delivery of large quantities of drug [10]. The delivery of large molecular weight monoclonal antibodies, that are usually required in high doses, requires a delivery strategy capable of providing high dose delivery. This particular issue provides a significant challenge for many of the solid and coated MN technologies, which are usually limited to low dose, potent agents such as vaccines [11]. As such, polymeric MN arrays can be used to deliver higher quantities of therapeutic agents.

In this work the aim was to compare and contrast the delivery of BEV using a hydrogel-forming MN platform and, independently, from a dissolving MN platform. This is the first example of a transdermal delivery system compatible with a biotherapeutic macromolecule of this molecular size. This work encompasses the formulation, characterisation and *in vitro* transdermal permeation of BEV from a hydrogel-forming MN platform and from a dissolving MN platform across excised neonatal porcine skin. Further, these two prototype MN platforms were tested *in vivo*, in Sprague-dawley rats assessing the serum concentrations of BEV and tissue concentrations of BEV in lymph nodes, spleen and skin tissues.

2. Materials and Methods

2.1 Chemicals

Avastin® concentrate solution for infusion 25 mg/ml was purchased from Roche, Welwyn Gaden City, Hertfordshire, UK. Cryogel SG3 was supplied by PB Gelatins, Pontypridd, UK. Pearlitol® 50C-Mannitol was supplied by Roquette, Lestrem, France. Sucrose was purchased from Sigma Aldrich, Dorset, UK. Sodium chloride (NaCl) was purchased from Sigma Aldrich, Steinheim, Germany. Sodium carbonate (Na_2CO_3) was purchased from Sigma Aldrich, Steinheim, Germany. Gantrez® S-97 was a gift from Ashland Pharmaceutical, Kidderminster, UK. PVA (MW 9,000-10,000 Da) was purchased from Sigma Aldrich, Steinheim, Germany. Nair™ Gentle hair removal cream was purchased from Nair Co., London, UK. Electric hair clippers were bought from Remmington Co., London, UK. Franz cell apparatus was purchased from Crown Glass Co. Sommerville, New Jersey, USA. Cyanoacrylate glue was purchased from Loctite® Dublin, Ireland. SpeedMixer™, DAC 150 FVZ-K was purchased from Synergy Devices Ltd., UK. Virtis Advantage® Bench top Freeze Drier System was purchased from SP Scientific, Warminster PA, USA. The patch occlusive (Scotchpak 9523) was purchased from 3M Carrickmines, Ireland. The occlusive layer was fixed to the MN patch using an adhesive (DuroTak™ 87-2100) which was purchased from National Starch & Chemical Company, Bridgewater, New Jersey, USA.

2.2 Pharmaceutical analysis of BEV in vitro and in vivo

The ELISA employed for the detection and quantification of BEV from *in vitro* sample matrices and *in vivo* Sprague-dawley rat serum matrices was validated in conjunction with the International Conference on Harmonisation of Technical Requirements for Registration of Pharmaceuticals for Human Use (ICH) Validation of Analytical Procedures Q2 Analytical Validation Revision one (R1) 2005. In summary, the primary coating antibody - recombinant human VEGF165 was diluted 1:5000 in 0.1M bicarbonate buffer (pH 9.6). 100 µl of the diluted recombinant human VEGF 165 solution was dispensed into each well, covered with Parafilm® and aluminium foil and incubated for 16 h at 4°C. The plate was washed with washing buffer, comprising of 0.05% v/v Tween®-20 in PBS (PBST), and left to soak for 30 s before being discarded. This process was repeated 5 times, following which the plate was dried briefly using absorbent paper. The plate was then blocked with SuperBlock® T20 for 2 h at room temperature. The plate was then washed with PBST, as described previously. A freshly

prepared BEV solution at a concentration of 1 mg/ml in PBS was prepared in the range of 400 ng/ml to 5 ng/ml for *in vitro* sample analysis and 400 ng/ml to 50 ng/ml for *in vivo* sample analysis. Samples were incubated for 1 h and then washed with PBST. The plate was incubated with the secondary antibody – biotinylated VEGF165 antibody diluted 1:10,000 in SuperBlock® T20 buffer for 1 h at room temperature and then washed with PBST. The plate was incubated with streptavidin-horseradish peroxidase (HRP) conjugate, diluted 1:5000 in PBS only, for 30 min at room temperature and again washed with PBST. The substrate 3,3',5,5'-tetramethylbenzidine (TMB) was added to each well and incubated for 30 min. Colour development was ended using 4.0 M hydrochloric acid and optical density (OD) was measured at 450 nm using a micro 96-well plate spectrophotometer (Powerwave XS, Bio-Tek Instruments Inc., London, UK.).

Correlation analysis with least squares linear regression analysis was performed on the calibration curves generated from both analytical methods, enabling determination of the equation of the line and their coefficients of determination. Limits of detection (LoD) and limits of quantification (LoQ) were determined using a method based on the standard deviation of the response and the slop of the representative calibration curve, as described in the guidelines from the ICH [12]. The LoD of each method was determined as follows, using Eq. (1):

$$\mathrm{Lod} = \frac{3.3\sigma}{\mathrm{S}}$$

Eq. (1)

where σ is the standard deviation of the response data used to construct the regression lines and S is the slope of that line. Subsequently, the LoQ was determined using Eq. (2):

$$\mathrm{LoQ} = \frac{10\sigma}{\mathrm{S}}$$

Eq. (2)

2.3 Stability studies of BEV in PBS

Standard solutions of BEV (250 µg/ml) in PBS were prepared by diluting BEV in PBS (pH 7.4) and these were stored under various conditions, namely: refrigerated to 4°C and protected from light, ambient temperature (20°C) and exposed to natural light, and heated using an incubator to 37°C and protected from light. These solutions were stored in 50 ml falcon tubes and samples taken at 0, 24, 48, and 72 h. A minimum of three replicates were stored in each case with 1 ml samples taken at each time point. The samples were subject to one complete freeze-thaw cycle prior to analysis by BEV specific ELISA, described below.

2.4 Formulation of dissolving MN arrays containing BEV

Dissolving MN arrays were prepared from aqueous blends of PVA and Avastin® concentrate solution for infusion. Initially an aqueous stock solution of PVA was prepared at 40% w/w. The PVA powder was mixed with water in a water bath at 40°C for 3 h, following which the formulation was allowed to stand for 12 h. The PVA stock solution was diluted with BEV and distilled water, to achieve a working concentration of 20% w/w PVA. This formulation was slowly mixed with a glass rod to ensure minimal bubble formation, and then centrifuged at 3500 rpm for 2 min. The formulation was dispensed onto prefabricated silicone moulds using a 1 ml standard syringe. The silicone moulds had an array of 19 x 19 pyramidal needles, each 500 µm high, 300 µm at the base with an interspacing of 50 µm. Gel formulation (100 µl) was dispensed onto each mould, of. Following this, the moulds were placed into a stainless steel positive pressure chamber and air was pumped into the vessel to increase atmospheric pressure to 3 bar. This pressure was maintained for 15 min to facilitate filling of the needle tips, the pressure was then reduced to normal atmospheric pressure and the moulds were removed from the chamber and allowed to dry at room temperature for 48 h. The dissolving MN arrays were then removed from the moulds, ready for use.

2.5 Formulation of hydrogel-forming MN arrays

Hydrogel-forming MN arrays were formulated from 20% w/w Gantrez® S-97, 7.5% w/w PEG 10,000 and 3% w/w Na_2CO_3. Firstly, an aqueous blend was obtained by fully dissolving Gantrez® S-97 and PEG 10,000 in water, following this Na_2CO_3 was added. This formulation was mixed well using a glass rod until foaming had ceased and a uniform gel was obtained. The formulation was then transferred into 50 ml falcon tubes and centrifuged for 15 min at

3500 rpm to remove bubbles. The formulation was dispensed onto prefabricated silicone moulds as described above. The hydrogel-forming MN arrays were cross-linked through an esterification reaction, by heating at 80°C for a further 24 h [13-15].

2.6 Formulation of lyophilised reservoirs containing BEV

Lyophilised drug reservoirs loaded individually with BEV were prepared following a previously developed lyophilisation process [14] . Briefly, BEV-containing reservoirs were formulated with 20% w/w Avastin® concentrate solution for infusion (25 mg/ml BEV) dissolved in distilled water. This was then added to a mixture containing 10% w/w gelatin, 40% w/w mannitol, 10% w/w NaCl and 1% w/w sucrose yielding a final mixture with 0.5% w/w BEV. The formulation was then mixed by a speed-mixer at 3000 rpm for 60 s and sonicated at 37°C for 60 min. The resulting formulation was then cast into 13 mm radius cylindrical moulds (250 mg) with one open end, frozen at −80°C for a minimum of 60 min and then lyophilised in a freeze-drier according to the following regime: primary drying for 48 h at a shelf temperature of −40°C, secondary drying for 10 h at a shelf temperature of 20°C and vacuum pressure of 50 mTorr.

2.7 Loss of mass following lyophilisation of BEV containing reservoirs

Low and high dose lyophilised wafers containing BEV were assessed for mass loss, as an indication of water loss following the lyophilisation process. Initially, approximately 250 mg of the wet formulation was cast into wafer moulds, with the exact mass recorded. Following lyophilisation, the wafers were de-moulded and weighed. Using Eq. (3), loss of mass as percentage was calculated as:

$$Loss\ of\ mass\ (\%) = \frac{M_w - M_d}{M_w} \times 100 \qquad \text{Eq. (3)}$$

where M_w is the mass of wet formulation cast into the wafer moulds and M_d is the mass of the dry wafer following lyophilisation.

2.8 MN insertion studies

Parafilm® was used as a model membrane to assess MN strength for penetration into the skin, as described previously by our Group [15]. Briefly, one sheet of Parafilm® was carefully folded, such that it formed 8 layers, approximately 1 mm thick. This was then laid onto a poly(ethylene) sheet for support. Manual insertion studies were conducted by applying thumb pressure to the MN array formulations. MN depth of penetration was assessed through visual inspection of the Parafilm® layers.

2.9 BEV recovery from lyophilised reservoirs

Low and high dose lyophilised wafers containing BEV were dissolved fully in 10 ml PBS (pH 7.4). A magnetic stirrer was used to ensure complete mixing, with the rotor set at 200 rpm, 20°C for 30 min. Following complete dissolution, samples were taken and analysed using the BEV specific ELISA.

2.10 BEV recovery from PVA dissolving MN

PVA MN arrays containing BEV were dissolved in 10 ml PBS (pH 7.4). A magnetic stirrer was used to ensure complete mixing, with the rotor set at 200 rpm, 20°C for 30 min. Following complete dissolution, samples were taken and analysed using BEV specific ELISA.

2.11 BEV MN mass

PVA MN arrays containing BEV were formulated and dry mass were recorded. The needle tips were then removed using a scalpel blade and baseplate mass recorded. The needle mass was calculated by subtracting the mass of arrays without needles from the mass of arrays with needles.

2.12 In vitro permeation studies of BEV on modified Franz cell apparatus

The permeation of BEV from lyophilised wafers though swelling hydrogel MN arrays and subsequently across neonatal porcine skin was investigated *in vitro* using modified Franz cell apparatus. FDC-400 Franz diffusion cells with flat flange, 15 mm luminal diameter, mounted on a FDCD diffusion drive console providing synchronized stirring at 600 rpm and receiver compartment temperature regulated at 37 ± 1ºC were used in this experimentation, as described previously [16]. Neonatal porcine skin was acquired from stillborn piglets and excised immediately (<24 h post-partum) and trimmed to 350 µm thickness using a

dermatome. The skin was stored at -20 ºC until it was needed. The neonatal porcine skin was shaved and equilibrated in PBS (pH 7.4) for 15 min prior to use. A portion of this skin was secured to the donor compartment of the diffusion cell using cyanoacrylate glue. MN arrays were applied to the skin using manual application pressure for 30 s. To facilitate adhesion of the lyophilised wafer, 10 µl of water was applied to the back of the MN array. A metallic weight was placed on top of the BEV containing lyophilised wafer to help maintain contact between wafer and MN, and also to ensure MN insertion throughout the 24-h experiment. A schematic representation of the Franz cell apparatus can be seen in Figure 3a.

The donor cell was secured to the receiver compartment using a steel clamp, and covered with Parafilm® to reduce evaporation. Samples were taken (<200 µl) at intervals over the 24 h time period with heat equilibrated PBS (pH 7.4) used to replace sampling fluid. Similarly, the permeation of BEV from dissolving PVA MN arrays was assessed using a similar Franz cell set-up. The MN arrays were manually inserted into the skin and a metallic weight was placed on top to ensure insertion was maintained. Again, samples were taken (<200 µl) at intervals over the 24 h time period with heat equilibrated PBS (pH 7.4) used to replace sampling fluid.

2.13 In vivo permeation studies of BEV in Sprague-dawley rats

Throughout the study, all animal experimentation was conducted in accordance with the policy of the federation of European Laboratory Animal Science Associations and the European Convention for the Protection of vertebrate animals used for experimental and other scientific purposes, with implementation of the principles of the 3 R's – replacement, reduction, and refinement. In each case, ethical permission for these animal experiments was obtained from the Queen's University Animal Welfare and Ethics Review Board. The Animals were anesthetised using isoflurane.

Dissolving MN arrays and hydrogel-forming MN arrays with lyophilised reservoirs containing BEV were applied to 10-week old, female, Sprague-dawley rats for *in vivo* assessment of transdermal drug delivery. The rats' backs were shaved and depilatory cream was applied to remove the hair 24 h prior to MN application. In the case of experiments carried out using BEV in lyophilised reservoirs, two cohorts were assessed namely HF-10 and HF-5. The HF-10 cohort received 4 hydrogel-forming MN arrays and 4 BEV loaded lyophilised wafers (each

containing 2.5 mg BEV) 10 mg in total (HF-10). The HF-5 cohort received 2 hydrogel-forming MN arrays and 2 BEV loaded lyophilised wafers (each containing 2.5 mg BEV) 5 mg in total (HF-5). The hydrogel-forming MN arrays were manually inserted into the hair free skin site on the rats' backs with the addition of a foam adhesive boarder to assist in application of the MN to the skin. An aliquot of 20 µl water was spotted onto the centre of each hydrogel-forming MN array and a lyophilised wafer placed on top of this. An adhesive film was applied onto and surrounding the MN system to aid in retention and provide adequate occlusion. Similarly, for experimentation involving dissolving MN arrays, the arrays were manually applied to hair free, clean dry skin on the rats' backs. In this instance only an adhesive film was applied in order to provide adequate retention of MN in the skin and appropriate occlusion. Three control rats were maintained throughout the experiment, receiving an initial IV dose of 100 µl of Avastin® *via* tail vein injection.

2.14 Serum extraction and processing

A maximum of 200 µl of blood was collected from the tail veins of the animals into a non-heparinised polypropylene 1.5 ml tube, following which the whole blood sample was placed in an incubator at 37°C for 40 min undisturbed, to facilitate clotting. The samples were then centrifuged at 4°C for 10 min at 2000 g, following which the supernatant (serum) was removed and placed into a clean dry non-heparinised polypropylene 1.5 ml tube and stored at -80°C. Each serum sample was subject to one complete freeze thaw cycle prior to analysis by ELISA.

2.15 Tissue sample extraction and processing

Skin samples from the MN site of application, exterior lumbar lymph nodes, axial lymph nodes and spleens were extracted *post-mortem* and processed for BEV concentration analysis by ELISA. The individual mass of each tissue sample was recorded, following which the samples were homogenised in known volumes of PBS (pH 7.4) using a VWR 200 Homogenizer unit. These samples were then analysed using the BEV specific ELISA and normalised to original sample mass.

2.16 Statistical analysis

Statistical analysis was performed using Microsoft® Excel® for Mac® 2016 and GraphPad® PRISM® 2016, and included calculation of mean, standard deviation, construction of

calibration plot with least squares linear regression analysis and analysis of residuals. Mann Whitney U, ANOVA and Student's t test were used as appropriate to assess statistical significance throughout. In all cases, $p<0.05$ denoted significance.

3. Results

3.1 Pharmaceutical analysis of BEV

Throughout this work, BEV was analysed through a BEV specific ELISA that was developed and validated to ICH standards. The limits of quantitation (LOQ) and detection (LOD) are presented in Table 1.

3.2 Stability studies of BEV in PBS

The stability of BEV in solution was monitored over a 72 h period, with samples subject to one complete freeze-thaw cycle. The percentage recovery of BEV when stored under varying conditions, namely: refrigerated at 4°C (dark), at ambient temperature 20°C (light), and heated to 37°C (dark) is shown in Figure 1.

At 0 h, BEV concentrations in PBS (pH 7.4) were determined to be 95.2 ± 5.48% of the original 250 μg/ml solution. At 72 h when stored at 37°C and protected from light, this dropped to 73.0 ± 14.5%. The lowest degree/amount of degradation was observed when samples were stored at 4°C and protected from light, showing a decrease to 81.0 ± 13.3%. Storing the solutions of BEV at 20°C and not protected from light led to a decrease to 73.1 ± 7.1% of the original concentration. The decrease in BEV recovery between 0 h and 72 h was of statistical significance (p = 0.0374), however there was no statistical difference in the decrease in percentage recovery post-72 h (p = 0.5793). This shows a similar trend to those samples stored at a higher temperature yet protected from light, suggesting photosensitivity could be the main cause of BEV degradation in PBS (pH 7.4) and that these effects may not be directly related to the increase in temperature. In subsequent experiments, BEV was refrigerated at 4°C, and protected from light.

3.2 Loss of mass experiments for MN drying and lyophilisation

Loss of mass was calculated for lyophilised reservoirs containing BEV as a result of dehydration upon freeze-drying. On average the BEV containing lyophilised reservoirs yielded a significant loss of mass of 33.0 ± 0.27% ($p < 0.05$). Similarly, the percentage water loss was documented for dissolving MN arrays following the drying process. On average the PVA dissolving MN arrays yielded a significant loss of mass of 65.9 ± 1.40% ($p < 0.05$).

3.3 MN insertion studies

In vitro insertion studies of dissolving MN arrays containing BEV and hydrogel-forming MN arrays into Parafilm® layers were carried out. The texture analyser was used to insert MN arrays uniformly into Parafilm® at a defined force of 32 N. Dissolving BEV MN tip heights were 497.0 ± 1.5 µm and 487.8 ± 3.1 µm before and after insertion, respectively. Hydrogel-forming MN tip heights were 503.8 ± 5.3 µm and 498.1 ± 3.5 µm before and after insertion, respectively. On average 99.7 ± 0.3% and 87.3 ± 11.4% of the 361 (19 x 19) hydrogel-forming MN inserted into the first and second layers of Parafilm®, with a significant drop to 12.2 ± 4.9% in the third layer (Figure 2).

A similar trend was observed with dissolving BEV MN with 100.0% needles penetrating the first layer of Parafilm®. The most significant decrease was seen between the percentage of needles inserting into the second and third layers of Parafilm® (78.0 ± 12.1% to 17.9 ± 5.6%). With each Parafilm® layer measuring 126 µm, penetration of needles to the third layer suggests the MN are inserting up to 378 µm of the total 500 µm height.

3.4 BEV recovery studies from lyophilised reservoirs and dissolving MN arrays

Lyophilised reservoirs containing BEV were dissolved in 10 ml PBS (pH 7.4). Samples were taken and percentage recovery was determined using BEV specific ELISA. Similarly, prior to the lyophilisation process, samples of the formulation were taken and percentage recovery was determined using BEV specific ELISA. The percentage recovery of BEV pre- and post-lyophilisation was 95.2 ± 3.33% and 92.7 ± 3.91%, respectively. BEV recovery from reservoirs pre- and post-lyophilisation was not statistically significant (p = 0.4457), indicating that the lyophilisation process had minimal impact upon the biological activity of BEV throughout the formulation process. Similarly, BEV recovery studies from dissolving PVA MN were carried out. Dry PVA MN arrays containing BEV were dissolved, samples were taken and percentage recovery was determined using BEV specific ELISA. Samples of the BEV-PVA gel formulation were taken and percentage recovery was determined using BEV specific ELISA. The percentage recovery of BEV pre- and post-drying was 90.2 ± 3.41% and 89.1 ± 4.13%, respectively. BEV recovery from PVA MN arrays pre- and post-drying was not statistically significant (p = 0.758) indicating that the drying process had minimal impact upon the biological activity of BEV throughout this formulation process.

3.5 Dissolving MN array needle tip and baseplate mass analysis

The weight of PVA MN arrays with and without needles was recorded, and the total needle weight calculated. The mean MN mass with and without needles was 34.1 ± 3.4 mg and 30.6 ± 3.0 mg respectively, making the proportion of MN array by mass encompassed by the needles alone was 2.4 ± 0.4%.

3.6 In vitro permeation studies

In vitro permeation of BEV across dermatomed neonatal porcine skin was conducted using a modified Franz cell apparatus setup. Lyophilised reservoirs were formulated such that the low dose contained 1250 µg BEV and the high dose contained 2500 µg BEV. The 24 h permeation profiles for high dose and low dose reservoirs in conjunction with hydrogel-forming MN arrays, compared to the control set-up (no MN) can be seen in Figure 3b.

The average MN-mediated permeation of BEV from high dose reservoirs was 687.8 ± 61.2 µg, equivalent to 27.5 ± 2.5% of available BEV (2500 µg), significantly more than the control release set up (p = 0.0238). The average MN-mediated permeation of BEV from low dose reservoirs was 303.4 ± 57.1 µg, which is equivalent to 24.3 ± 4.6% of available BEV (1250 µg). This was also of statistical significance compared to the control set-up (p = 0.0357). Permeation of BEV from the control set-up (no MN) was 24.5 ± 21.1 µg, or 0.9 ± 0.8% of available BEV (2500 µg). It should be noted that the control permeation results lay below the limit of detection of the BEV specific ELISA and, therefore, can only serve to indicate that a very low concentration of BEV had permeated after 24 h. The difference between MN-mediated low and high dose permeation of BEV after 24 h was also of statistical significance (p = 0.0043), showing almost a two-fold increase in permeation. This doubling effect strongly indicates a dose dependent mechanism of permeation from the lyophilised reservoirs, through the hydrogel-forming MN arrays and skin, into the receiver compartment of Franz cell apparatus.

Similar *in vitro* permeation studies were conducted using dissolving PVA MN arrays containing BEV. In this instance, dissolving MN arrays were formulated to contain 1250 µg BEV in each array. The lower drug loading is one of the drawbacks of formulating a dissolving MN array.

In this case the drug loading is limited by the amount of polymer gel loaded into the MN moulds. The permeation profile of BEV from PVA dissolving MN arrays can be seen in Figure 3c.

The mean permeation of BEV from dissolving PVA MN arrays after 24 h was 105.2 ± 11.9 μg, which is equivalent to 8.7 ± 0.9% of the total BEV available (1250 μg). It is worth noting that the needles comprised 10.4 ± 0.4% of the total array by mass. Taking into account the large molecular weight of BEV it could be assumed that there would be minimal diffusion of BEV from the baseplate, and in fact only polymer and drug in the needles would be delivered. With this in mind, it is perhaps more realistic to imagine that only 10% of the total BEV loading, equivalent to the drug loading in the needles would be available for delivery. Assuming approximately 125 μg of BEV in the needle tips, permeation of 105.2 ± 11.9 μg represents approximately 84 ± 9.5% of the available BEV after 24 h.

3.7 In vivo delivery of BEV in Sprague-dawley rats

In vivo delivery of BEV was conducted in female Sprague-dawley rats aged 10 weeks. A four-way comparison study was undertaken, comparing high and low dose delivery of BEV from lyophilised reservoirs through hydrogel-forming MN arrays, dissolving PVA MN arrays containing BEV and IV control. In this study the HF-10 (hydrogel-forming 10 mg) cohort received 4 hydrogel-forming MN arrays with 4 accompanying lyophilised reservoirs, each containing 2500 μg BEV (total 10 mg BEV). The HF-5 (hydrogel-forming 5 mg) cohort received 2 hydrogel-forming MN arrays with 2 accompanying lyophilised reservoirs, each containing 2500 μg BEV (total 5 mg BEV). The PVA-5 (PVA dissolving MN) cohort received 4 arrays applied to each rat, each containing 1250 μg BEV (total 5 mg BEV). The IV control cohort received one dose of 100 μl of Avastin® 25 mg/ml concentrate for infusion through tail IV injection, totalling 2.5 mg BEV.

The MN formulations were applied to the backs of shaved rats using manual application technique for 3 min and held *in situ* for 24 h using an occlusive adhesive patch and surgical tape (shown in Figure 4A). Blood samples were taken at defined intervals for one week, serum was extracted and stored at -80°C, undergoing one freeze thaw cycle prior to ELISA analysis. Following removal of the PVA-5 dissolving MN from the rat's backs after 24 h, in each case

the array needle baseplate had dissolved completely, as shown in Figure 4B. In both the HF-10 and HF-5 cohort, following removal of the hydrogel-forming MN arrays from the rats back at 24 h, microchannels were clearly visible (Figure 4C) and the MN arrays had swollen extensively with the lyophilised reservoirs having dissolved fully (Figure 4D).

Figure 5 shows the mean serum concentrations of BEV over the course of one week, as quantified by BEV specific ELISA.

Figure 5 shows that the IV control cohort consistently displayed the highest serum concentrations of BEV with the peak serum concentration (C_{max}) observed soon after the initial administration (75.6 µg/ml at 4 h). At 24 h the serum concentration had reduced to 42.7 ± 70.1 µg/ml and by the end of the experimental time period the serum concentration was 28.4 ± 6.1 µg/ml (168 h). The C_{max} for IV control was statistically different to HF-10, HF-5, and PVA-5 C_{max} ($p < 0.0001$).

Following the extraction of exterior lumbar and axial lymph nodes, skin tissue samples and spleens, BEV concentrations were determined and are shown in Figure 6.

It can be seen that the BEV concentration in the exterior lumbar lymph nodes at 168 h shows no significant difference between hydrogel-forming MN, dissolving MN and IV treatment groups (p= 0.2463). However, in comparison, the BEV concentrations found in the axial lymph nodes shows a significant difference, with the IV control cohort significantly higher than the other MN treated cohorts (p<0.0001). In contrast to this, there was no significant difference between BEV concentrations in the skin, at the site of MN application at 168 h (p=0.2579). Looking at the spleen tissue concentrations, the IV control group display a significantly higher BEV concentration, compared to the other MN treated rats (p<0.0001).

The BEV serum concentration at steady state was calculated for HF-10, HF-5, and PVA-5 using Equation 4 below, where AUC is the area under the curve and t is time.

$$Css = \frac{AUC_{0-t}}{t} \qquad \text{Eq (4)}$$

The pharmacokinetic parameters for HF-10, HF-5 and PVA-5 platforms are summarized in Table 2.

The HF-5 cohort consistently yielded the lowest serum concentrations of the various delivery platforms. The time of maximum serum concentration (T_{max}) was observed at 48 h yielding 81.2 ± 25.2 ng/ml with serum concentrations reducing to 56.7 ± 5.7 ng/ml at 168 h. The HF-5 C_{max} was statistically different from HF-10 and PVA-5 C_{max} (p = 0.100). The HF-10 cohort displayed a similar serum concentration profile. However, it was consistently higher than seen in the HF-5 platform. Similar to the HF-5 platform, the T_{max} was 48 h (358.2 ± 100.4 ng/ml). The experimental endpoint of 168 h yielded a serum concentration that had decreased to 210.7 ± 6.3 ng/ml. Although the HF-10 C_{max} was statistically different to the HF-5 and IV control C_{max}, the difference with PVA-5 C_{max} was not significant (p = 0.200). In contrast to the HF-10 and HF-5 platforms, the PVA-5 dissolving arrays showed the T_{max} at the 6 h time point, with C_{max} of 488.7 ng/ml. However, due to the limitations with respect to repeated blood sampling in rats, this data point is representative of only one rat blood sample and is therefore of minimal significance. The serum concentration at 24 h was 403.5 ± 88.9 ng/ml for the PVA-5 platform and by 168 h had decreased to 149.6 ± 21.1 ng/ml. It is interesting to see that in the HF-10 and HF-5 cohorts the T_{max} was observed almost 24 h after the MN array had been removed from the back of the rats, suggesting that a main aspect of controlled delivery conferred by this system lies between BEV entering the microcirculation and progressing to the circulating serum within the rat. This is in contrast to the PVA-5 cohort, where T_{max} is seen much earlier.

4. Discussion

Since the development of recombinant technologies, pharmaceutical formulators have struggled to provide delivery options for these structurally complex molecules, other than through parenteral injection. Currently, biologically-selective therapeutics such as monoclonal antibodies, are restricted to the traditional hypodermic needle and syringe model. Alternative drug delivery options may be afforded through MN-mediated transdermal platforms. Indeed, a number of biotherapeutic agents have been delivered across the skin using MN technology – insulin, growth hormone, model protein compounds such as ovalbumin and bovine serum albumin [17-20]. Dissolving MN arrays penetrate the skin and, following hydration of the polymer chains in the interstitial skin fluid, begin to dissolve, releasing polymer and drug. Hydrogel-forming MN arrays provide an aqueous pathway from drug reservoir to the dermal microcirculation through penetration of the upper skin layers and subsequent *in situ* swelling. This work looks at the potential for hydrogel-forming MN arrays and dissolving MN arrays to facilitate delivery of a large macromolecule, such as BEV (MW = 149,000 Da). Transdermal delivery of BEV may provide an alternative method for administration which could provide opportunities for drug delivery by use of a minimally invasive technology.

Initially short term degradation studies were conducted in order to assess the effect of light and heat on the recovery of BEV from aqueous solutions. It is well documented that biotherapeutic agents such as antibodies containing aromatic amino acid residues can absorb UV-light. This in turn can result in the conversion of amino acid side chains, altering the molecular structure of the compound and as such can have conformational effects on the overall folding and tertiary structure. [21][22]. In this instance BEV degradation from Avastin® was not further increased by exposure to light, however, this may be a consideration for prolonged storage. Multi-domain protein molecules, such as BEV are subject to degradation upon heating, and as such BEV remain in a conformational naïve state in higher concentrations when stored at lower temperatures [23]. This brief analysis indicated that in order to attain high recovery of BEV from solution, protection from UV-light and cooled conditions would be required.

The lyophilisation process was shown not to result in excessive degradation of BEV, yielding high percentage recovery. Lyophilisation is now routinely used within the biopharmaceutical manufacturing sector, as it has shown to be a stable format for protein formulation [25]. The concept of a lyophilised drug reservoir has previously been shown to be a viable option for formulation of biomolecules, such as the model compound ovalbumin [7]. Similarly, the gel formulation, casting and drying of PVA-BEV into MN arrays showed minimal degradation upon recovery analysis. This is an encouraging feature of MN preparation, with potential for minimal losses in high value therapeutics during the formulation stages. Loss of active therapeutic throughout manufacture is of prime concern to industrial partners when considering scale-up and commercialisation of a novel drug delivery platform, such as with MN technology. It has been noted that dissolving and hydrogel-forming MN arrays may require specific packaging to ensure that changes in atmospheric humidity do not affect needle strength and integrity [26]. Therefore, the use of appropriate packaging, such as heat-sealed moisture impermeable foils, could provide an acceptable option for primary packaging of dissolving or hydrogel-forming MN array products. A further consideration of MN packaging relates to the maintenance of MN integrity and insertion in skin. Larraneta *et al*. in 2014 described a novel method for MN skin penetration modelling using readily available laboratory film [15]. Replicating these studies, the MN insertion studies conducted here suggest that both hydrogel-forming MN and dissolving BEV MN were successfully inserted *in vitro*.

In vitro permeation of BEV from drug-loaded dissolving MN arrays and a combined system of hydrogel-forming MN arrays and drug loaded lyophilised reservoirs was assessed using Franz cell apparatus. Here, excised neonatal porcine skin is used as the model membrane. While it is recognised that porcine skin is not an exact model of human skin, it has been documented that the *SC* closely matches the hair density and thickness [27]. The *SC* is known to act principally as the main barrier to drug permeation, and so in this case is thought to serve as an appropriate model of human skin. The limited permeation of BEV from the high dose control lyophilised wafer (no MN) demonstrates the limited ability for BEV to cross intact skin. BEV is a large molecule which may restrict its permeation by passive diffusion through skin. Dissolution of BEV loaded lyophilised wafers is complete within 15 min when tested in PBS alone. With this in mind, the permeation controlling feature of this combined system is likely

to relate to the swelling of the hydrogel-forming MN arrays [10]. The permeation of BEV from the hydrogel-forming system represents 27.5 ± 2.5% and 24.3 ± 4.6% of available BEV in the high and low dose reservoirs, respectively. Previously conducted studies with model proteins such as ovalbumin have shown percentage permeation rates of 49% [10]. The lower percentage permeation observed in the current study may be as a result of slower diffusion of such a large molecule through the tortuous hydrogel network. The hydrodynamic radius of a monoclonal antibody such as BEV (Mw = 149,000 Da) is clearly much larger than that of a model protein compound such as ovalbumin (Mw = 45,000 Da) and so slower permeation could be expected. It appears that the BEV system has delivered its full payload by 6 h and so may not be suitable for 24 h patch application time. With respect to PVA dissolving MN arrays, in the dry state these can penetrate the *SC* and almost immediately begin to dissolve in interstitial fluid. As the polymer chains hydrate and dissolve the BEV is released from the needle tips. This BEV is then able to permeate through the skin and into the receiver compartment. In contrast to the hydrogel-forming system, we see only 8.7 ± 0.9% of total BEV delivered from PVA MN. The needles comprise approximately 10% w/w of the dry MN array (needles and baseplate). Low permeation of this nature suggests that only BEV contained in the MN needles themselves is available for delivery, with minimal or no movement of BEV contained in the baseplate. Compare this to previous work conduced with small molecule therapeutics such as ibuprofen, where a small proportion of the baseplate containing drug was able to permeate through the microchannel caused by the MN arrays before the skin seals over, and an alternative mechanism of release could be suggested [28]. The large sterically hindered BEV molecule may not be as “mobile” as other small molecules, such as ibuprofen, and so as the baseplate/needle interface begins to hydrate and dissolve the BEV is unable to move through the microchannels prior to skin closure. This ultimately may restrict delivery of large biotherapeutic molecules from dissolving MN to the amount of drug that can be incorporated into the needles themselves. A two-step manufacturing process whereby drug-containing gel is cast into the MN tips alone, and subsequently fused to a blank baseplate may help improve the delivery efficiency from this MN system. A two-step procedure for the manufacture of dissolving MN arrays containing drug only in the needle tips has previously been reported [29].

This *in vivo* study in rats represents one of the first examples of successful delivery of a clinically relevant biotherapeutic macromolecule using an integrated system of hydrogel-

forming MN arrays and lyophilised drug reservoir. This study also provides an opportunity to compare and contrast BEV delivery from a hydrogel-forming system and a dissolving MN platform. Antibody delivery from dissolving MN array platforms have been reported in the literature. Recently a dissolving MN system for the delivery of anti-PD1 antibody for cancer immunotherapy was described by Wang *et al.* [30]. Similar dissolving MN platforms have also been described by Chen *et al.* [31]. These publications demonstrate the capacity for dissolving MN arrays to provide transdermal delivery of biotherapeutic macromolecules however, there is currently no published work showing the efficacy of hydrogel-forming MN as a transdermal delivery system for antibody therapeutics such as BEV. With respect to the hydrogel-forming MN system, following removal of the arrays post-24 h, it was apparent that the MN had swollen extensively, with almost full dissolution of the lyophilised reservoirs in each case. In some of the patches, a white residue could be seen on the surface of the MN arrays. However, in the majority of cases the MN array had become opaque where the lyophilised reservoir had dissolved and moved into the hydrogel matrix itself. This suggests that the swollen MN arrays provided sufficient fluid to dissolve the lyophilised reservoir, allowing it to fulfil its purpose of delivering BEV into and through the MN array. During the 24 h experiment, the rats were highly mobile, despite this however the swollen MN arrays remained in place. A number of patient acceptability studies have shown that patients would prefer to wear a MN patch over receiving a hypodermic injection [32]. Similarly, with the PVA-5 cohort, upon return post-24 h application the MN arrays had dissolved fully with only a small quantity of baseplate gel remaining on the site of application. Although both needles and baseplates had dissolved upon removal, it is unlikely that significant quantities of BEV had diffused through the microchannels produced by the MN, despite these channels remaining open for some time after the MN have penetrated the *SC*. Comparing *in vitro* dissolution of PVA MN arrays, the needle tips dissolved within 5 h. Therefore, it may be reasonable to assume similar dissolution kinetics *in vivo*. It remains that minimal permeation of BEV from the baseplate may be expected due to its large hydrodynamic volume and potential to be retarded by steric hindrance.

It is interesting to note that the serum concentrations continued to rise after the HF-10 and HF-5 MN had been removed from the rat's backs. This suggests that the rate limiting stage of drug delivery may not be directly as a result of the swelling kinetics of the hydrogel-forming

MN arrays, rather BEV diffusion within the skin itself. Although *in vitro* permeation studies showed a high degree of mobility of BEV from lyophilised reservoir into the skin and ultimately into the receiver compartment, the peak serum concentrations do not appear at 6 h as expected. Instead, C_{max} is not seen until the 48 h sample, 24 h after the hydrogel-forming MN system has been removed from the rats' backs. Without more regular blood sampling it is impossible to say that 48 h time point represents the true T_{max}. However, it may be reasonable to assume T_{max} is reached between 24-48 h. This delay in serum concentration peak suggests that BEV is not entering to the circulating blood from the dermal microcirculation, and is either being retained within the skin layers to be leached out slowly, or flushed to the lymphatic system prior to re-entry to circulating blood. BEV has an isoelectric point of 7.6 and so when resident in the interstitial skin fluid (neutral pH) it is likely that BEV is predominantly positively charged [33]. BEV may be interacting with negatively charged molecules resident in the skin layer, such as glycosaminoglycans, resulting in the observed delay in BEV C_{max}. In comparison with the hydrogel-forming platform, BEV released from the dissolving PVA platform may be protected by the polymer chains from interacting with negatively charged molecules, and so helping to explain the faster absorption observed in this study.

It is known that small molecules such as water, glucose, and ions can passively move through the endothelial lining of blood vessels. However, larger molecules such as albumin, IgG and other antibodies cannot [34]. Molecules with a molecular radius of >3.6 nm (IgG ~ 11.5 nm) are predominantly transported *via* transcytosis or vesicular transport [35]. Transcellular transport is significantly slower than the passive diffusion of smaller molecules and, so, may be less favoured by BEV. It is anticipated that significant quantities of BEV are flushed from the dermal interstitium to the draining lymphatic system. This pathway may help to explain the delay in BEV entering to the circulating blood. With specific reference to the exterior lumbar and axial lymph, spleen and skin tissue, BEV was quantified in the lymphatic system. The presence of BEV here supports our suggestion that transdermal delivery of BEV, and possibly other large biomolecules could permeate from the skin in this way. In order to understand fully the pathway taken by BEV from interstitial skin fluid to circulating blood volume, further studies involving radiolabelled antibodies could be used to trace these macromolecules as they pass through the lymphatic system [36]. With respect to PVA-5

dissolving platform, the T_{max} is observed considerably sooner at 6 h. Such a difference in observed T_{max} between the hydrogel-forming and dissolving platforms exemplifies the potentially different mechanism of BEV permeation. In this instance, as PVA is a hydrophilic polymer, there is minimal delay in BEV release as the needles can immediately begin to dissolve upon insertion [37]. With respect to the hydrogel-forming system, dissolution and permeation of BEV can only begin once the array has begun to swell and sufficient fluid is available to begin reservoir dissolution. The comparatively higher C_{max} observed following PVA-5 application may result from rapid dissolution of the MN in skin and as such releasing the full available payload of BEV from the needle tips as a bolus dose. In contrast to this the HF-10 and HF-5 platforms may more slowly release their BEV cargo over the 24 h period leading to a lower C_{max} and broader pharmacokinetic profile.

In comparison to the IV control, based on this data, the transdermal options have not provided equivalent circulating serum concentrations. However, without further testing it is impossible to say that high concentrations of BEV are not in other tissue compartments, such as in the lymphatic system. It stands to reason that a molecule of such a large hydrodynamic radius may be more likely to be transported by the draining lymphatic fluid, rather than permeate directly into the blood stream. This may provide an option for MN-mediated transdermal, targeted delivery of macromolecules to the lymphatic system. It is well documented that the lymphatic system plays a key role in the spread of metastases following primary cancer development [38]. This may have implications for the treatment of lymphoma carcinoma or secondary metastasis following a number of primary cancers, where the targeting of monoclonal antibody medicines to particular tissue compartments within the body could be beneficial.

Serum concentrations of BEV following IV administration were equivalent to the recommended human circulating concentrations of BEV. A number of clinical efficacy studies have shown that the effect of receiving 5 mg/kg every 2 weeks in humans can result in a circulating concentration of ~50 μg/ml with >98% of VEGF bound to BEV yielding significant inhibition. Any further increase in BEV dosing would result in only minor additional inhibition of circulating VEGF [39]. On this occasion, the circulating BEV serum concentrations provided by PVA-5, HF-5 and HF-10 were sub-clinical. However, this work provides robust evidence that

transdermal delivery of a biotherapeutic macromolecule such as BEV can be achieved using dissolving MN and hydrogel-forming MN technology. It is unlikely that extending the application time of the dissolving PVA MN would yield further delivery of BEV. Similarly, extending the application time of hydrogel-forming MN would unlikely provide further delivery. As previously stated, limiting BEV to the needle tips in the dissolving platforms may improve delivery efficiency and reduce therapeutic wastage. It is important to consider all possibilities early in the commercialisation process with regards to for the development of new medical devices, such as MN arrays. It may, therefore be beneficial to include both aspects of dissolving and hydrogel-forming technologies into a combined patch. This may provide opportunities for the sustained release of a biotherapeutic macromolecule such as BEV, based on this work, up to 48 h. Initial bolus dosing could be delivered from dissolving needles and prolonged release of BEV could be provided from hydrogel-forming needles. In both cases, there is much scope for patch scale-up, as these experiments were conducted using 0.5 cm^2 MN arrays. Both polymeric and hydrogel-forming MN arrays have been proposed for use in humans at patch sizes of up to 30 cm^2. Patches of this size have been manufactured at bench scale by a number of research groups [13,40] and would provide significant opportunities for increasing the transdermal dose of BEV delivered, but would require further *in vivo* analysis.

5. Conclusion

Transdermal delivery of clinically relevant quantities of biotherapeutic macromolecules, such as antibodies, using MN has not yet been possible. Here dissolving and hydrogel-forming MN arrays have been formulated and used to by-pass the skin's barrier function and deliver BEV systemically. This work stands as proof-of-principle evidence for the transdermal delivery of antibody therapeutics using polymeric MN arrays. BEV was detected and measured in plasma across 7 days following one single application of MN arrays. BEV was also detected in lymph nodes, spleen and skin tissues suggesting lymphatic accumulation *in vivo*. The delivery of antibody therapeutics, specifically to the lymphatic system, could prove to be a viable option for treatment of lymphomas and secondary metastatic tumours. Opportunities for circumventing some of the problems associated with traditional hypodermic needle and syringe methods may be overcome by use of polymeric MN arrays. This work provides an insight into the delivery mechanisms of dissolving and hydrogel-forming MN platforms in rats. With further optimisation and alteration, it is conceivable that a MN system combining both dissolving and hydrogel-forming technologies could result in effective delivery of BEV and other biotherapeutic macromolecules, at controlled rates, using the skin as the principal route of delivery.

6. Data Availability

The raw/processed data required to reproduce these findings cannot be shared at this time as the data also forms part of an ongoing study.

7. References

[1] A. Beck, L. Goetsch, C. Dumontet, N. Corvaia, Strategies and challenges for the next generation of antibody-drug conjugates, Nat. Rev. Drug Discov. 16 (2017) 315–337.

[2] European Medicines Agency, Bevacizumab: Summary of Product Characteristics, 2005.

[3] R. Genentech, Avastin - bevacizumab, (2016). http://www.avastin.com (accessed 29 July 2016).

[4] X. Zhong, P. Neumann, M. Corbo, E. Loh, Recent Advances in Biotherapeutics Drug Discovery and Development, in: Drug Discov. Dev. - Present Futur., 2011.

[5] A.L. Daugherty, R.J. Mrsny, Formulation and delivery issues for monoclonal antibody therapeutics, Adv. Drug Deliv. Rev. 58 (2006) 686–706.

[6] R. Respaud, L. Vecellio, P. Diot, Nebulization as a deliivery method for mAbs in respiratory diseases, Expert Opin. Drug Deliv. 12 (2015) 1027–1039.

[7] R.F. Donnelly, M.T.C. McCrudden, A.Z. Alkilani, E. Larraneta, E. McAlister, A.J. Courtenay, M.C. Kearney, T.R. Raj Singh, H.O. McCarthy, V.L. Kett, E. Caffarel-Salvador, S. Al-Zahrani, A.D. Woolfson, Hydrogel-forming microneedles prepared from 'super swelling' polymers combined with lyophilised wafers for transdermal drug delivery, PLoS One. 9 (2014).

[8] N.G. Rouphael, M. Paine, R. Mosley, S. Henry, D. V. McAllister, H. Kalluri, W. Pewin, P.M. Frew, T. Yu, N.J. Thornburg, S. Kabbani, L. Lai, E. V. Vassilieva, I. Skountzou, R.W. Compans, M.J. Mulligan, M.R. Prausnitz, The safety, immunogenicity, and acceptability of inactivated influenza vaccine delivered by microneedle patch (TIV-MNP 2015): A randomised, partly blinded, placebo-controlled, phase 1 trial, Lancet. 6736 (2017) 1–10.

[9] X. Zhao, J.C. Birchall, S.A. Coulman, D. Tatovic, R.K. Singh, L. Wen, F. Susan Wong, C.M. Dayan, S.J. Hanna, Microneedle delivery of autoantigen for immunotherapy in type 1 diabetes, J. Control. Release. 223 (2016) 178–187.

[10] R.F. Donnelly, M.T.C. McCrudden, A. Zaid Alkilani, E. Larrañeta, E. McAlister, A.J. Courtenay, M.-C. Kearney, T.R.R. Singh, H.O. McCarthy, V.L. Kett, E. Caffarel-Salvador, S. Al-Zahrani, a D. Woolfson, Hydrogel-forming microneedles prepared from 'super

swelling' polymers combined with lyophilised wafers for transdermal drug delivery., PLoS One. 9 (2014) e111547.

[11] Y. Ma, W. Tao, S.J. Krebs, W.F. Sutton, N.L. Haigwood, H.S. Gill, Vaccine Delivery to the Oral Cavity Using Coated Microneedles Induces Systemic and Mucosal Immunity, Pharm. Res. (2014) 1–11.

[12] ICH, International conference on harmonisation of technical requirements for registration of pharmaceuticals for human use, in: ICH Harmon. Tripart. Guid. Anal. Proced. Text Methodol., 2005.

[13] R.F. Donnelly, T.R.R. Singh, M.J. Garland, K. Migalska, R. Majithiya, C.M. McCrudden, P.L. Kole, T.M.T. Mahmood, H.O. McCarthy, a D. Woolfson, Hydrogel-Forming microneedle arrays for enhanced transdermal drug delivery., Adv. Funct. Mater. 22 (2012) 4879–4890.

[14] M.T.C. McCrudden, A.Z. Alkilani, A.J. Courtenay, C.M. McCrudden, B. McCloskey, C. Walker, N. Alshraiedeh, R.E.M. Lutton, B.F. Gilmore, A.D. Woolfson, R.F. Donnelly, Considerations in the sterile manufacture of polymeric microneedle arrays., Drug Deliv. Transl. Res. 5 (2015) 3–14.

[15] E. Larrañeta, J. Moore, E.M. Vicente-Pérez, P. González-Vázquez, R. Lutton, a. D. Woolfson, R.F. Donnelly, A proposed model membrane and test method for microneedle insertion studies, Int. J. Pharm. 472 (2014) 65–73.

[16] K. Migalska, D.I.J. Morrow, M.J. Garland, R. Thakur, a. D. Woolfson, R.F. Donnelly, Laser-engineered dissolving microneedle arrays for transdermal macromolecular drug delivery, Pharm. Res. 28 (2011) 1919–30.

[17] K. Cheung, T. Han, D.B. Das, Effect of force of microneedle insertion on the permeability of insulin in skin., J. Diabetes Sci. Technol. 8 (2014) 444–452.

[18] M.B. Delgado-Charro, R.H. Guy, Effective use of transdermal drug delivery in children, Adv. Drug Deliv. Rev. 73 (2014) 63–82.

[19] K. van der Maaden, E.M. Varypataki, S. Romeijn, F. Ossendorp, W. Jiskoot, J. Bouwstra, Ovalbumin-coated pH-sensitive microneedle arrays effectively induce ovalbumin-specific antibody and T-cell responses in mice., Eur. J. Pharm. Biopharm. 88 (2014) 310–5.

[20] Y.K. Demir, Z. Akan, O. Kerimoglu, Sodium alginate microneedle arrays mediate the transdermal delivery of bovine serum albumin, PLoS One. 8 (2013) e63819.

[21] J. Haywood, O. Mazziconacci, K. Allegre, B. Kerwin, C. Schoneich, Light-induced conversion of Trp to Gly and Gly hydroperoxide in IgG1, Mol. Pharm. 10 (2013) 1146–1150.

[22] S. Singh, J. Zhang, C. O'Dell, M. Hsieh, J. Goldstein, J. Liu, Effect of polysorbate 80 quality on photostability of a monoclonal antibody, AAPS Pharm. Sci. Technol. 13 (2012) 422–430.

[23] A. Vermeer, W. Norde, The thermal stability of immunoglobulin: unfolding and aggregation of a multi-domain protein, Biophys. J. 78 (2000) 394–404.

[24] A.W.P. Vermeer, W. Norde, A. Van Amerongen, The Unfolding / Denaturation of Immunogammaglobulin of Isotype 2b and its F ab and F c Fragments, Biophys. J. 79 (2000) 2150–2154.

[25] M. Cicerone, M. Pikal, K. Qian, Stabilization of proteins in solid form, Adv. Drug Delovery Rev. 93 (2015) 14–24.

[26] P.A. McCarron, A.D. Woolfson, R.F. Donnelly, G.P. Andrews, A. Zawislak, J.H. Price, Influence of plasticizer type and storage conditions on properties of poly(methyl vinyl ether-co-maleic anhydride) bioadhesive films, J. Appl. Polym. Sci. 91 (2004) 1576–1589.

[27] M.J. Garland, K. Migalska, T.-M. Tuan-Mahmood, T. Raghu Raj Singh, R. Majithija, E. Caffarel-Salvador, C.M. McCrudden, H.O. McCarthy, a David Woolfson, R.F. Donnelly, Influence of skin model on in vitro performance of drug-loaded soluble microneedle arrays., Int. J. Pharm. 434 (2012) 80–9.

[28] M.T.C. Mccrudden, A.Z. Alkilani, C.M. Mccrudden, E. McAlister, H.O. McCarthy, A.D. Woolfson, R.F. Donnelly, Design and physicochemical characterisation of novel dissolving polymeric microneedle arrays for transdermal delivery of high dose, low molecular weight drugs, J. Control. Release. 180 (2014) 71–80.

[29] J. McCaffrey, C.M. McCrudden, A.A. Massey, J.W. McBride, M.T. McCrudden, E.M. Vicente-Perez, J.A. Coulter, T. Robson, R.F. Donnelly, H.O. McCarthy, Transcending epithelial and intracellular biological barriers: a prototype DNA delivery device, J. Control. Release. 226 (2016) 238–47.

[30] C. Wang, Y. Ye, G.M. Hochu, H. Sadeghifar, Z. Gu, Enhanced Cancer Immunotherapy by Microneedle Patch-Assisted Delivery of Anti-PD1 Antibody., Nano Lett. 16 (2016) 2334–40.

[31] J. Chen, Y. Qiu, S. Zhang, Y. Gao, Dissolving microneedle-based intradermal delivery of

interferon-α-2b., Drug Dev. Ind. Pharm. 9045 (2015) 1–7.

[32] S. Marshall, L.J. Sahm, A.C. Moore, Microneedle technology for immunisation: Perception, acceptability and suitability for paediatric use, Vaccine. 34 (2016) 723–734.

[33] H. Wiig, O. Tenstad, Interstitial exclusion of positively and negatively charged IgG in rat skin and muscle., Am. J. Physiol. Heart Circ. Physiol. 280 (2001) H1505-12.

[34] S. Sukriti, M. Tauseef, P. Yaazbeck, D. Mehta, Mechanisms regulating endothelial permeability, Pulm. Circ. 4 (2014).

[35] Y. Komarova, A. Malik, Regulation of endothelial permeability via paracellular and transcellular transport pathways, Annu. Rev. Biophys. 72 (2010) 463–93.

[36] G.A.M.S. Van Dongen, A.J. Poot, D.J. Vugts, PET imaging with radiolabeled antibodies and tyrosine kinase inhibitors: Immuno-PET and TKI-PET, Tumor Biol. 33 (2012) 607–

[37] C. chan Wang, F. lin Yang, L.F. Liu, Z. min Fu, Y. Xue, Hydrophilic and antibacterial properties of polyvinyl alcohol/4-vinylpyridine graft polymer modified polypropylene non-woven fabric membranes, J. Memb. Sci. 345 (2009) 223–232.

[38] S. Karaman, M. Detmar, Mechanics of lymphatic metastasis, J. Clin. Invest. 124 (2014).

[39] European Medicines Agency, Bevacizumab Scientific Discussion, (2005) 1–61. http://www.ema.europa.eu/docs/en_GB/document_library/EPAR_-_Scientific_Discussion/human/000582/WC500029262.pdf.

[40] H. Kathuria, H. Li, J. Pan, S.H. Lim, J.S. Kochhar, C. Wu, L. Kang, Large Size Microneedle Patch to Deliver Lidocaine through Skin, Pharm. Res. 33 (2016) 2653-67.

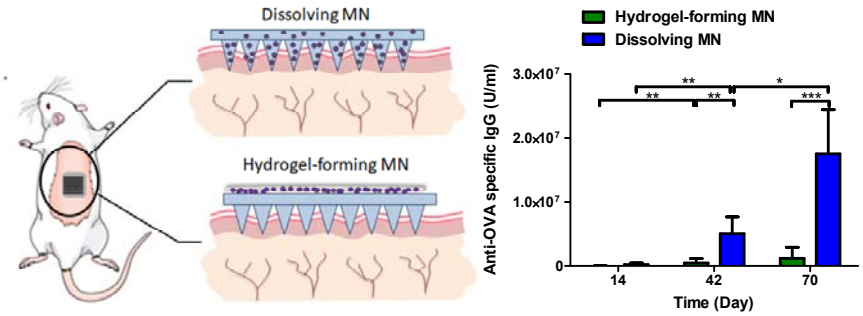

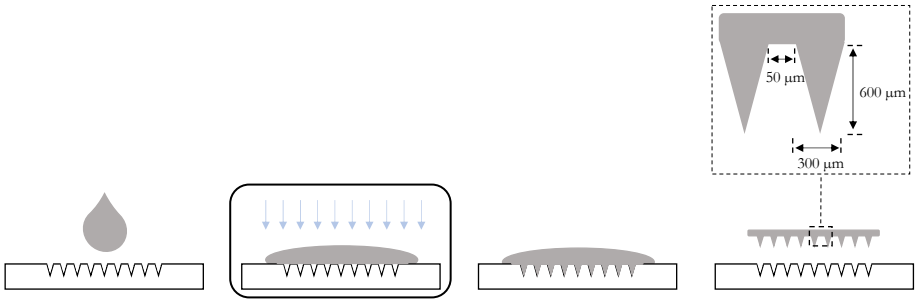

A. Dispense formulation B. Positive pressure environment C. Drying D. MN array removal

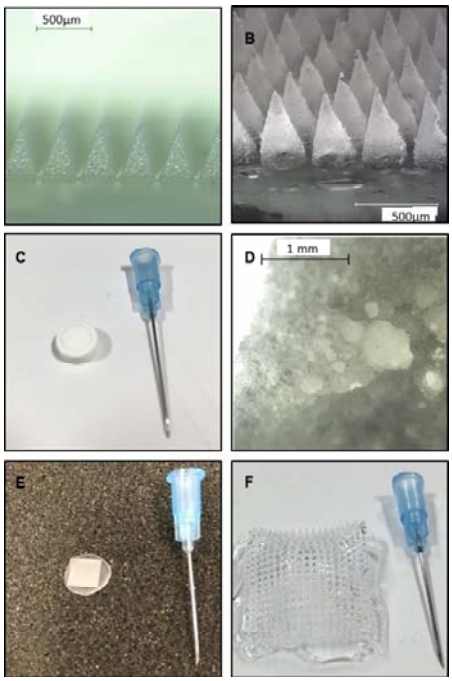
500µm
B
500µm
C
D
1 mm
E
F

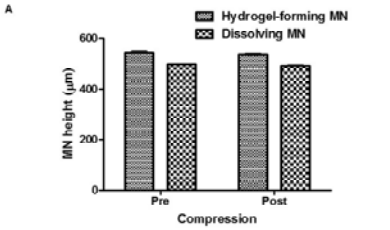
A
Hydrogel-forming MN
Dissolving MN
MN height (µm)
600
400
200
0
Pre
Post
Compression

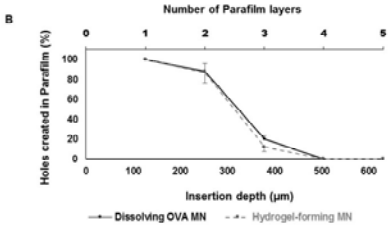
B
Number of Parafilm layers
0
1
2
3
4
5
Holes created in Parafilm (%)
100
80
60
40
20
0
0
100
200
300
400
500
600
Insertion depth (µm)
Dissolving OVA MN
Hydrogel-forming MN

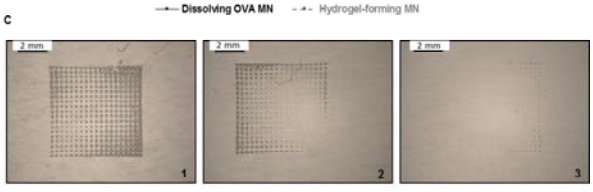
C
2 mm
1
2 mm
2
2 mm
3

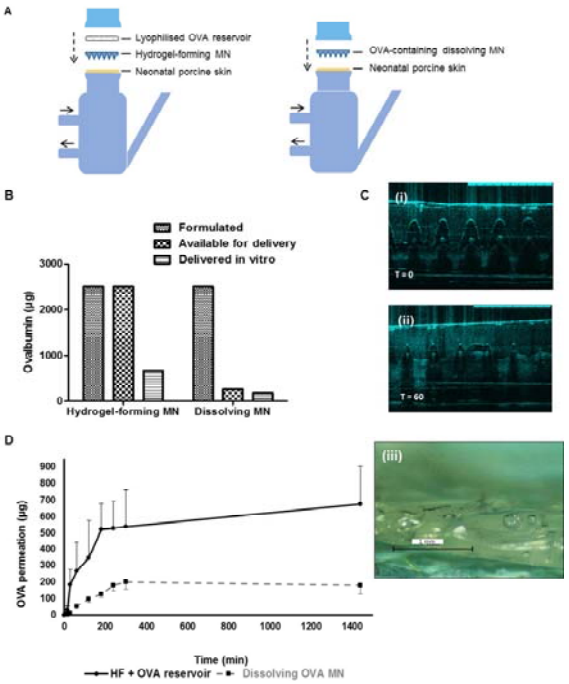
A
Lyophilised OVA reservoir
Hydrogel-forming MN
Neonatal porcine skin
OVA-containing dissolving MN
Neonatal porcine skin
B
Formulated
Available for delivery
Delivered in vitro
Ovalbumin (μg)
3000
2000
1000
0
Hydrogel-forming MN
Dissolving MN
C
(i)
T = 0
(ii)
T = 60
D
OVA permeation (μg)
900
800
700
600
500
400
300
200
100
0
0
200
400
600
800
1000
1200
1400
Time (min)
HF + OVA reservoir
Dissolving OVA MN
(iii)

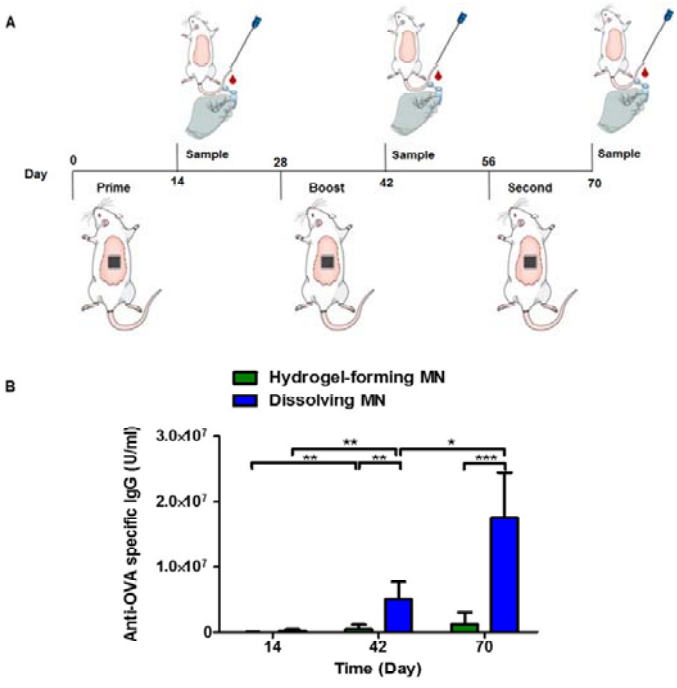
A
Day
0
Sample
14
28
Sample
42
56
Sample
70
Prime
Boost
Second
B
Hydrogel-forming MN
Dissolving MN
Anti-OVA specific IgG (U/ml)
3.0x10^7
2.0x10^7
1.0x10^7
0
**
**
**
*
***
14
42
70
Time (Day)